HAL
open science

# The Snake River Plain Experiment revisited. Relationships between a Farallon plate fragment and the transition zone

Éric Beucler, Sébastien Chevrot, Jean-Paul Montagner

## To cite this version:

Éric Beucler, Sébastien Chevrot, Jean-Paul Montagner. The Snake River Plain Experiment revisited. Relationships between a Farallon plate fragment and the transition zone. Geophysical Research Letters, 1999, 26 (17), pp.2673-2676. 10.1029/1999GL008345 . hal-03196234

**HAL Id: hal-03196234**

**https://nantes-universite.hal.science/hal-03196234v1**

Submitted on 12 Apr 2021

**HAL** is a multi-disciplinary open access archive for the deposit and dissemination of scientific research documents, whether they are published or not. The documents may come from teaching and research institutions in France or abroad, or from public or private research centers.

L'archive ouverte pluridisciplinaire **HAL**, est destinée au dépôt et à la diffusion de documents scientifiques de niveau recherche, publiés ou non, émanant des établissements d'enseignement et de recherche français ou étrangers, des laboratoires publics ou privés.

GEOPHYSICAL RESEARCH LETTERS, VOL. 26, NO. 17, PAGES 2673-2676, SEPTEMBER 1, 1999

# The Snake River Plain experiment revisited. Relationships between a *Farallon* plate fragment and the transition zone

Eric Beucler, Sébastien Chevrot[1] and Jean-Paul Montagner

Laboratoire de sismologie globale, I.P.G.P., France

**Abstract.** We reconsider the analysis of the 93 PASSCAL-OREGON SRP experiment data. The techniques applied to the processing of *Pds* waves, which are *P* to *S* conversions at seismic discontinuities at depth *d* in the receiver region, differ from those employed by *Dueker & Sheehan* [1997]. We perform global moveout corrections and migration, taking advantage of the alignment of seismicity along the great circle described by the array (South America, and the Kuril and Aleutians islands). We do not detect a deep signature of a mantle plume. The 410 km discontinuity exhibits a fragmented aspect, which prevents us from reliably estimating the transition zone thickness. The 660 km discontinuity is clearly more visible, and largely deflected in a large part of the profile. We associate this anomalous behaviour and the noisy aspect of the discontinuities with the presence of a *Farallon* plate fragment.

## Introduction

Lateral variations of body wave velocities are closely related to mineralogical compositions and temperature. The seismic discontinuities at the nominal depths of 410 and 660 km ("410" and "660") are usually attributed to the phase transformations of olivine and/or pyroxene. While recent studies display small variations of the transition zone thickness on a global scale [*Chevrot et al.*, 1999], large topography variations of the 410 and the 660 have been reported on a regional scale study using an array of 20 broadband stations in the Yellowstone-Snake River Plain (YSRP) complex [*Dueker & Sheehan*, 1997]. The array configuration was a 510 km NW-SE trending line crossing the YSRP (Fig. 1), which is assumed to be the Yellowstone hotspot track [*Smith & Braile*, 1994]. Indeed, while a part of the magmatic material is trapped in the lithosphere under the actual Yellowstone caldera, producing high siliceous lavas, the plume is sheared by the North-American plate motion. We analyze the data produced by the 93 PASSCAL-OREGON SRP experiment in order to detect the *P* to $S_V$ converted phases. We present a 2D cross section of the upper mantle beneath the YSRP complex and examine the relations between our results and different tomographic models of North America [*van der Lee & Nolet*, 1997a; *Grand et al.*, 1997].

## Data processing

Over the course of the 6-month experiment, 344 earthquakes of magnitude larger than 5 were recorded by the 20 broadband seismometers. We only consider events whose back-azimuths are very close to the great circle described by the array (Fig. 1). To avoid complications due to triplications on transition zone discontinuities, we only select epicentral distances larger than 30°. We fix the threshold for the maximum amplitude of $S_V$ in the *P* wave coda at 15 % of the maximum amplitude of the *P* wave. After a careful inspection of all available seismograms, only 260 $S_V$ components matched these criteria. All records are band-pass filtered between 8 and 50 seconds. Each seismogram is then projected on

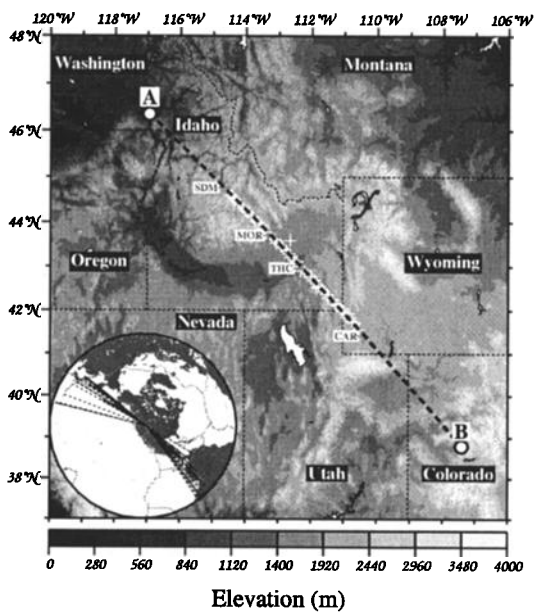


**Figure 1.** Western US topography and 93 PASSCAL-OREGON SRP broadband stations array. During the 6-month experiment the 20 stations occupied different sites (white crosses). State borders are given in solid lines and the SRP is the topographic depression west of the Yellowstone hotspot (symbolised by the large Y). The segment [AB] (dashed line) is the trace of the vertical cross section (Fig. 4). Back-azimuths distribution used in this study figures in the inserted panel.

[1]Now at Dept of Earth, Atmospheric and Planetary Sciences, M. I. T., Cambridge, USA.

Copyright 1999 by the American Geophysical Union.

Paper number 1999GL008345.
0094-8276/99/1999GL008345$05.00

the $(P, S_V, S_H)$ axes. To remove the complications related to the source time function, $S$ components are deconvolved from the $P$ waveform pulse. Then, we apply several techniques, including moveout corrections, stack and migration algorithms adapted to detect conversions at deep discontinuities.

### 1D study

The 260 $S_V$ components are first stacked together with moveout corrections [*Vinnik*, 1977]. We choose a reference epicentral distance of 66.5°, which corresponds to a ray parameter value of 6.4 s.deg$^{-1}$ in our reference velocity model (IASP91) [*Kennett & Engdahl*, 1991]. Stacking is performed every 30 km from 0 to 750 km depth. If the appropriate moveout corrections are applied, stacking at the right depth and at the right time shift enhances the phases present in the records.

The stacks are presented in figure 2, where the time scale is relative to the $P$ wave arrival. The phases present in the first 35 s are principally formed by reflections and conversions from $P$ to $S_V$ waves in the crust. In particular, the large phase ~4 s after the $P$, is the $Pms$ phase, a conversion at the Moho discontinuity. The phases between 10 and 35 s are multiply reflected waves on crustal discontinuities [*Dueker & Sheehan*, 1997]. The maxima energies for $P410s$ and $P660s$ in figure 2 are localised respectively at 46.68 ± 0.31 s and 70.77 ± 0.36 s. Thus, the mean travel time across the transition zone is 24.09 ± 0.47 s, which is close to the global average obtained by *Chevrot & al.* [1999]. This first approach shows that the transition zone thickness is normal, at the scale of the array.

In order to explore if smaller scale variations are present, we separately stack NW and SE back-azimuths receiver functions. Moveout corrections are computed every kilometer for each ray path and also for the reference one. Then, we interpolate each time correction value with the corresponding reference time shift. In other words, we project all wave travel paths along the reference one. For each station, we stack every corrected seismogram and sort the resulting stacks by station latitude. To improve the spatiotemporal coherence a moving average over 5 adjacent stations is performed. The two images in figure 3 display the result which can be seen as a two dimensional view of the upper mantle discontinuities distorted along the reference ray path for each back-azimuth family.

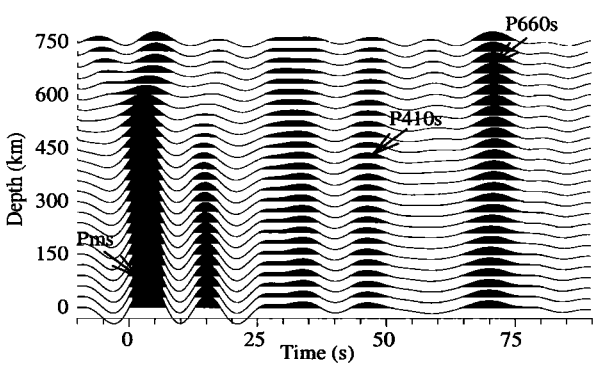


**Figure 2.** Stacked $S_V$ components. Each seismogram corresponds to a trial depth of conversion between 0 and 750 km depth. Records are stacked every 30 km depth, applying the theoretical moveouts for a converted phase originating at this depth. Time is relative to $P$ wave at 0 s. Arrows point on the energy corresponding to the theoretical $Pds$ phases.

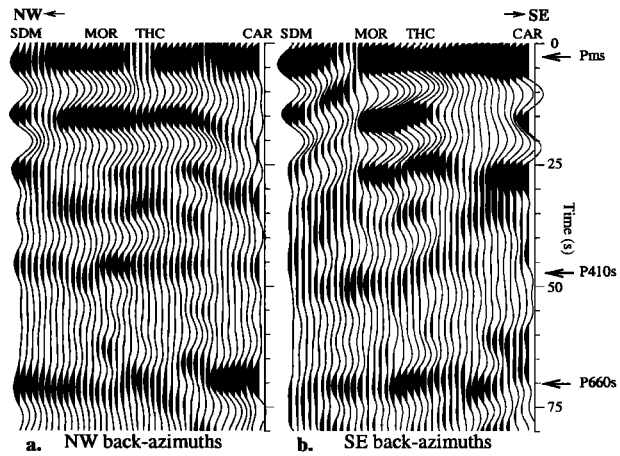


**Figure 3.** *Pds* moveout curves for the NW (a) and the SE (b) back-azimuths. Each seismogram represents the stack of all traces recorded by a single station, after moveout corrections applied and projected along the reference wave path. The two figures are smoothed by a moving average over 5 stations.

The $Pms$ phases seem to vanish where the array crosses the SRP (between stations THC and MOR). After focusing on this region using a band-pass filter between 2 and 50 s, we detected two phases which destructively interfer when the data are low-pass filtered at 8 s. This conversion source has been already detected [*Sparlin et al.*, 1982; *Peng & Humphreys*, 1997] and interpreted as a cooled magmatic reservoir formed when the North-American plate crossed over the Yellowstone hotspot 8 Ma ago. The $P410s$ phases are horizontal to the NW part of the profile (Fig. 3a), but vary dramatically to the SE (Fig 3b). The $P660s$ phases are better detected. In figure 3a, we notice a converted phase crossing the 660 from the NW dipping to the SE. The large delay time of this phase excludes a crustal origin and its dipping aspect is not consistent with the topography of a 520 km discontinuity [*Shearer*, 1996]. Since the two images (Fig. 3a and 3b) sample the mantle beneath the array differently, the contrast between them is not necessarily incompatible.

### 2D study

To assess the discontinuities topography and constrain the anomalous converted phase observed in figure 3a, the 260 seismograms are migrated into spatial image of the upper mantle beneath the segment [AB], a 1100 km long cross section (Fig. 1). After discretizing the medium into 20 km wide and 10 km thick boxes,

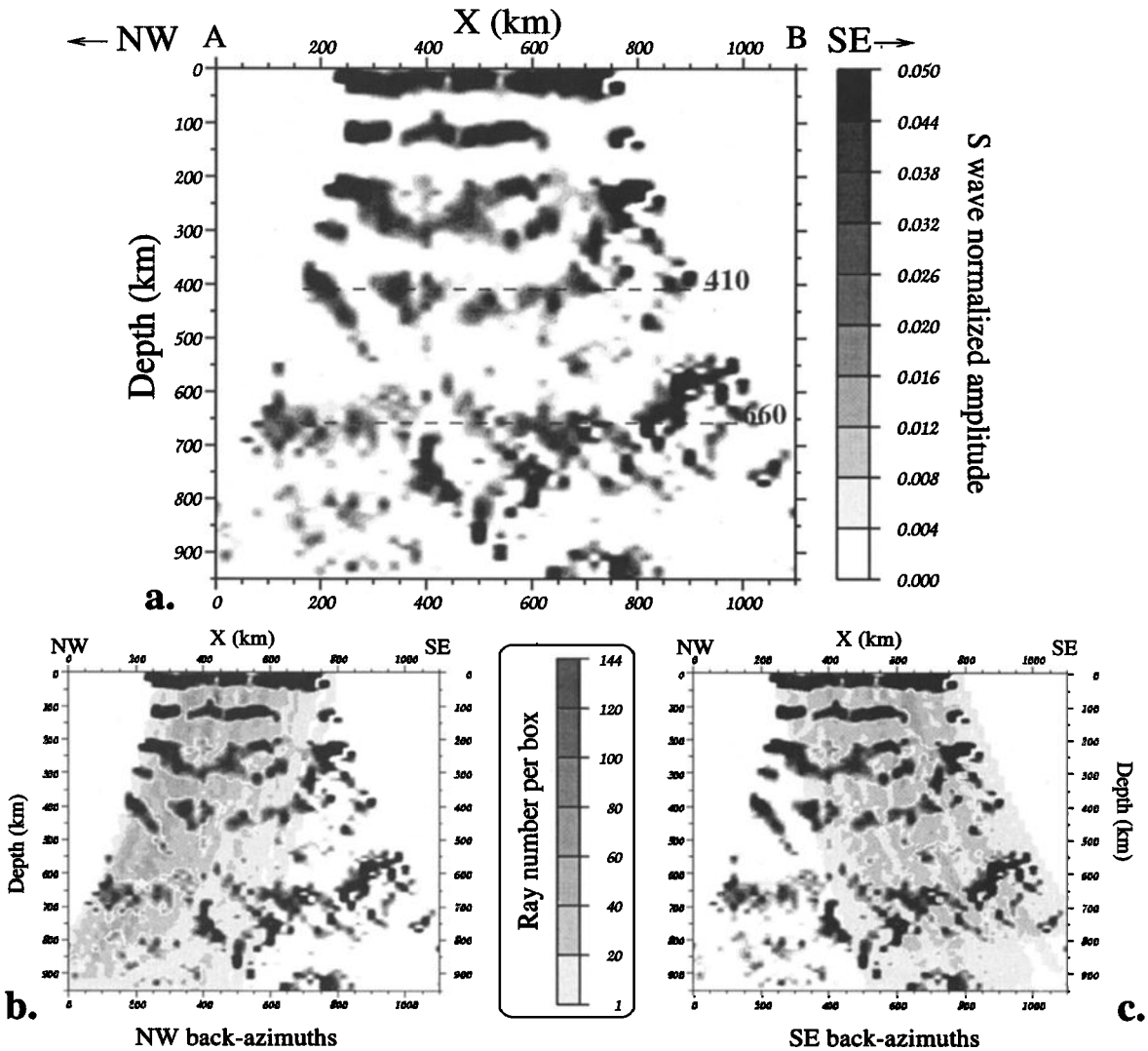


**Figure 4.** (a) Upper mantle discontinuity structure beneath the [AB] segment (Fig. 1), obtained by migration. Each box is 20 km wide and 10 km thick. Value in each box corresponds to the average of all amplitudes collected in this box. (b) NW and (c) SE rays density overlaid by migration result.

receiver functions are back projected from the station to the conversion sources through these boxes. All the amplitude values collected in one box are averaged and we only consider boxes which were hit by more than 10 rays.

*Dueker & Sheehan* [1997] computed stacks of all the traces that hit 75 km wide bins, separated by 25 km, at two given depths (400 and 700 km). The two stacks were then merged to form a trace for each bin location. Thus, different paths were mixed together into a one dimensional stacked trace. In comparison, our image represents a real two dimensional view of all possible conversion interfaces.

The migration image is displayed in figure 4a, the 0 km depth corresponds to the *P* wave arrival. The 410 is fragmented and not really highlighted. The 660 signature is much more obvious but reveals some singular variations in its topography. In the very SE part of the section (Fig. 4a), a rapidly varying aspect prevents from any conclusion on the transition zone thickness. Approximately 450 km to the SE of A, the topography of the 660 is unclear. It could either be interpreted as a 60 km upward deflection or as a downward deflection of ~150 km.

In order to estimate the behaviour of the migration near the boundaries of each ray set, we produced two images representing the ray distributions of NW and SE back-azimuths overlaid by the migration result (Fig. 4b and 4c). We first note that the area where both NW and SE back-azimuths rays overlap is located within the first 500 km depth. Second, many structures display a large sensitivity to the ray distribution. Consequently, we must use caution when interpreting the structures aligned with the edges of the NW or the SE ray coverage. Thus, the 150 km downwelling of the 660 is certainly biased because of a bad focusing of the mi-

gration. The most robust observation is the presence of two inclined conversion interfaces between 450 and 750 km depth, in the NW part of the profile, which are not related to any ray distribution. These two structures with a 55° apparent dip could correspond to the converted phase already detected in figure 3a.

## Discussion and conclusion

In order to estimate if IASP91 could influence the resolution of our migration image (Fig. 4a), we perform the same migration operation using a 2D velocity model built from a vertical cross section along the same segment [AB] (Fig. 1) in the NA95$S$ model [*van der Lee & Nolet*, 1997a], which provide the best resolution for the first 400 km depth. No significant differences between both migration results are observed except a change of the apparent depth of the discontinuities, which is hardly visible on the migrated section. Cross sections in two $S$ wave velocity models [*van der Lee & Nolet*, 1997b; *Grand et al.*, 1997] display an abnormal fast velocity in the NW part. This high velocity anomaly is explained by the presence of the subducting *Farallon* plate or at least fragments of it. The dipping phases detected in figure 4a could be related to the conversions on the slab edges. The water released by the dehydration of a diving plate could broaden the discontinuities above and thus explain the discontinuous aspect of the 410 [*Wood*, 1995]. Nevertheless, relations between the dipping structure and the upper mantle discontinuities remains ambiguous because of the noisy aspect of the image. The 60 km uplift of the 660 previously mentionned would be inconsistent with the presence of a cold slab and a negative Clapeyron slope for the phase transformation at this discontinuity [*Bina & Helffrich*, 1994]. Another possible explanation could be that we are observing the interactions between the subducting slab and the 660. In this hypothesis, the uplift could be related to the accretion of fertilized peridotite which cannot penetrate into the lower mantle [*Ringwood*, 1994].

In conclusion, considering our resolution, we detect no evidence of a mantle plume signature at depth. The comparison with tomographic models [*van der Lee & Nolet*, 1997b; *Grand et al.*, 1997], suggests that the dipping structures could be related to a *Farallon* plate fragment. Interaction between the medium and this slab results in a fragmented aspect of the upper mantle discontinuities, which prevents us from making any reliable estimate of the variation of the transition zone thickness beneath the array. Thus, we find little support in the data to the highly anomalous variations of the transition zone thickness reported by *Dueker & Sheehan* [1997]. The 660 behaviour is quite complex but the thick slab interaction model [*Ringwood*, 1994] could provide a plausible explanation. Indeed, although Clapeyron slopes demonstrate that the presence of a cold body would elevate the 410 and depress the 660, kinetic effects of a slab while diving may also bring an important contribution to the discontinuities topography. We realize that our interpretations may be highly speculative. Nevertheless, we feel that such an approach, applied on better quality data sets, may provide some interesting insights into the detailed structure of the transition zone in the near future.

**Acknowledgments.** We are grateful to E. Humphreys for making the data of the 93 PASSCAL SRP experiment available to us and for sending preprints before publication. We would like to thank also L. Vinnik for helpful discussions.

## References

Bina, C.R. and G. Helffrich, Phase transition Clapeyron slopes and transition zone seismic discontinuity topography, J. Geophys. Res., *97*, 4791-4807, 1994.

Chevrot, S., L.P. Vinnik and J.P. Montagner, Global patterns of upper mantle from Ps converted phases, J. Geophys. Res., in press, 1999.

Dueker, K.G. and A.F. Sheehan, Mantle discontinuity from midpointstacks of converted $P$ to $S$ waves across the Yellowstone hotspot track, J. Geophys. Res., *102*, 8313-8327, 1997.

Grand, S.P. and R. van der Hilst and S. Widiyantoro, Global seismic tomography: A snapshot of convection in the Earth, GSA Today, *7*, 1-7, 1997.

Kennett, B. and E. Engdahl, Travel times for global earthquake location and phase identification, Geophys. J. Int., *105*, 429-465, 1991.

Peng, X. and E.D. Humphreys, Crustal velocity structure across the eastern Snake River Plain and the Yellowstone swell, J. Geophys. Res., *103*, 7171-7186, 1998.

Ringwood, A.E., Role of the transition zone and 660 km discontinuity in mantle dynamics, Phys. Earth Planet. Int., *56*, 5-24, 1994.

Shearer, P.M., Transition zone velocity gradients and the 520-km discontinuity, J. Geophys. Res., *101*, 3053-3066, 1996.

Smith, R.B. and L.W. Braile, The Yellowstone hotspot, Journal of Volcanology and Geothermal Res., *61*, 121-187,1994.

Sparlin, M.A., L.W. Braile and R.B. Smith, Crustal structure of the eastern Snake River Plain determined from ray trace modelling of seismic refraction data, J. Geophys. Res., *87*, 2619-2633, 1982.

van der Lee, S. and G. Nolet, Upper mantle $S$ velocity structure of North America, J. Geophys. Res., *102*, 22815-22838, 1997a.

van der Lee, S. and G. Nolet, Seismic image of the subducted trailing fragments of the Farallon plate, Nature, *286*, 266-269, 1997b.

Vinnik L.P., Detection of waves converted from $P$ to $S_V$ in the mantle, Phys. Earth Planet. Int., *15*, 39-45, 1977.

Wood B.J., The effect of $H_2O$ on the 410-kilometer seismic discontinuity, Science, *268*, 74-76, 1995.

E. Beucler, S. Chevrot, J.P. Montagner. Laboratoire de sismologie globale, I.P.G.P., 4 place Jussieu, 75252 Cedex 05 Paris, FRANCE. (e-mail: beucler@ipgp.jussieu.fr, chevrot@ipgp.jussieu.fr, jpm@ipgp.jussieu.fr)

(Received April 5, 1999; revised June 10, 1999; accepted July 16, 1999 .)